

Published in final edited form as:

Nature. 2012 August 2; 488(7409): 100–105. doi:10.1038/nature11284.

ICGC PedBrain: Dissecting the genomic complexity underlying medulloblastoma

David TW Jones^{1,*}, Natalie Jäger^{2,*}, Marcel Kool¹, Thomas Zichner³, Barbara Hutter², Marc Sultan⁴, Yoon-Jae Cho⁵, Trevor J Pugh⁶, Volker Hovestadt⁷, Adrian M Stütz³, Tobias Rausch³, Hans-Jörg Warnatz⁴, Marina Ryzhova⁸, Sebastian Bender¹, Dominik Sturm¹, Sabrina Pleier¹, Huriye Cin¹, Elke Pfaff¹, Laura Sieber¹, Andrea Wittmann¹, Marc Remke¹, Hendrik Witt^{1,9}, Sonja Hutter¹, Theophilos Tzaridis¹, Joachim Weischenfeldt³, Benjamin Raeder³, Meryem Avci⁴, Vyacheslav Amstislavskiy⁴, Marc Zapatka⁷, Ursula D Weber⁷, Qi Wang², Bärbel Lasitschka¹⁰, Cynthia C Bartholomae¹¹, Manfred Schmidt¹¹, Christof von Kalle¹¹, Volker Ast¹², Chris Lawerenz¹², Jürgen Eils¹², Rolf Kabbe², Vladimir Benes¹³, Peter van Sluis¹⁴, Jan Koster¹⁴, Richard Volckmann¹⁴, David Shih¹⁵, Matthew J Betts¹⁶, Robert B Russell¹⁶, Simona Coco¹⁷, Gian Paolo Tonini¹⁷, Ulrich Schüller¹⁸, Volkmar Hans¹⁹, Norbert Graf²⁰, Yoo-Jin Kim²¹, Camelia Monoranu²², Wolfgang Roggendorf²², Andreas Unterberg²³, Christel Herold-Mende²³, Till Milde^{9,24}, Andreas E Kulozik⁹, Andreas von Deimling^{25,26}, Olaf Witt^{9,24}, Eberhard Maass²⁷, Jochen Rössler²⁸, Martin Ebinger²⁹, Martin U Schuhmann³⁰, Michael C Frühwald³¹, Martin Hasselblatt³², Nada Jabado³³, Stefan Rutkowski³⁴, André O von Bueren³⁴, Dan Williamson³⁵, Steven C Clifford³⁵, Martin G McCabe^{36,37}, V. Peter Collins³⁷, Stephan Wolf¹⁰, Stefan Wiemann^{10,38}, Hans Lehrach⁴, Benedikt Brors², Wolfram Scheurlen³⁹, Jörg Felsberg⁴⁰, Guido Reifenberger⁴⁰, Paul A Northcott¹⁵, Michael D Taylor⁴¹, Matthew Meyerson^{6,42}, Scott L Pomeroy^{6,43}, Marie-Laure Yaspo⁴, Jan O Korbel³, Andrey Korshunov^{25,26}, Roland Eils^{2,44,#}, Stefan M Pfister^{1,9,#}, and Peter Lichter^{7,#} on behalf of the ICGC PedBrain Tumor Project⁴⁵

¹Division of Pediatric Neurooncology, German Cancer Research Center (DKFZ), Im Neuenheimer Feld 280, Heidelberg, 69120, Germany ²Division of Theoretical Bioinformatics, German Cancer Research Center (DKFZ), Im Neuenheimer Feld 280, Heidelberg, 69120, Germany ³European Molecular Biology Laboratory (EMBL), Meyerhofstrasse 1, Heidelberg, 69117, Germany ⁴Max Planck Institute for Molecular Genetics, Ihnestr. 63-73, Berlin, 14195, Germany ⁵Division of

Correspondence and requests for materials should be addressed to: R.E. (r.eils@dkfz-heidelberg.de), S.M.P. (s.pfister@dkfz-heidelberg.de), or P.L. (m.macleod@dkfz-heidelberg.de).

*These authors contributed equally

#These authors contributed equally

Supplementary Information is linked to the online version of the paper at www.nature.com/nature.

Author Contributions

D.T.W.J., M.Su., A.M.S., H-J.W., S.B., S.P., H.C., E.P., L.S., A.W., S.H., T.T., B.R., C.C.B., M.Sch., C.v.K., V.B., R.V., S.Wo., S.Wi., and J.F. performed and/or coordinated experimental work.
N. Jäger, D.T.W.J., M.K., T.Z., B.H., M.Su., T.P., V.Ho., T.R., H-J.W., J.W., M.A., V.Am, M.Z., Q.W., B.L., V.Ast, C.L., J.E., R.K., P.v.S., J.K., D.Sh., M.J.B., R.B.R. and P.A.N. performed data analysis.
Y-J.C., M.Ry., M.Re., S.C., G.P.T., U.S., V.Ha., N.G., Y-J.K., C.M., W.R., A.U., C.H-M., T.M., A.E.K., A.v.D., O.W., E.M., J.R., M.E., M.U.S., M.C.F., M.H., N.Jabado, S.R., A.O.v.B., D.W., S.C.C., M.G.M., V.P.C., W.S., G.R., M.D.T., and A.K. collected data and provided patient materials.
D.T.W.J., N.Jäger, D.St., M.K., V.Ho., H.W., R.E., S.M.P. and P.L. prepared the initial manuscript and figures.
U.D.W., H.L., B.B., G.R., M.M., S.L.P., M-L.Y., J.O.K., R.E., A.K., S.M.P., and P.L. provided project leadership.
All authors contributed to the final manuscript

Author Information Short-read sequencing data have been deposited at the European Genome-phenome Archive (EGA, <http://www.ebi.ac.uk/ega/>) hosted by the EBI, under accession number EGAS00001000215. Reprints and permissions information is available at www.nature.com/reprints. The authors declare no competing financial interests. Readers are welcome to comment on the online version of this article at www.nature.com/nature.

Child Neurology, Stanford University, 750 Welch Road, Palo Alto, CA, 94304, USA ⁶Broad Institute of MIT and Harvard, Cambridge, MA, 02142, USA ⁷Division of Molecular Genetics, German Cancer Research Center (DKFZ), Im Neuenheimer Feld 280, Heidelberg, 69120, Germany ⁸Department of Neuropathology, NN Burdenko Neurosurgical Institute, 4th Tverskaya-Yamskaya 16, Moscow, 125047, Russia ⁹Department of Pediatric Oncology, Hematology & Immunology, Heidelberg University Hospital, Im Neuenheimer Feld 430, Heidelberg, 69120, Germany ¹⁰Genomics and Proteomics Core Facility, German Cancer Research Center (DKFZ), Im Neuenheimer Feld 280, Heidelberg, 69120, Germany ¹¹Division of Translational Oncology, German Cancer Research Center (DKFZ) and National Center for Tumor Diseases (NCT), Im Neuenheimer Feld 460, Heidelberg, 69120, Germany ¹²Data Management Facility, German Cancer Research Center (DKFZ), Im Neuenheimer Feld 280, Heidelberg, 69120, Germany ¹³Genomics Core Facility, European Molecular Biology Laboratory (EMBL), Meyerhofstrasse 1, Heidelberg, 69117, Germany ¹⁴Department of Oncogenomics, AMC, University of Amsterdam, Meibergdreef 9, Amsterdam, 1105 AZ, Netherlands ¹⁵The Arthur and Sonia Labbatt Brain Tumor Research Centre, Hospital for Sick Children, 555 University Avenue, Toronto, Ontario, M5G 1X8, Canada ¹⁶Cell Networks Cluster of Excellence, University of Heidelberg, Heidelberg, 69120, Germany ¹⁷Department of Advanced Diagnostic Technologies, IRCCS Azienda Ospedaliera Universitaria San Martino - IST Istituto Nazionale per la Ricerca sul Cancro, L.go R. Benzi, 10, Genoa, 16132, Italy ¹⁸Center for Neuropathology and Prion Research, University of Munich, Feodor-Lynen-Strasse 23, Munich, 81377, Germany ¹⁹Institute for Neuropathology, Evangelisches Krankenhaus, Remterweg 2, Bielefeld, 33617, Germany ²⁰Department of Paediatric Oncology and Haematology, Saarland University Hospital, Homburg, 66421, Germany ²¹Institute for Pathology, Saarland University Hospital, Kirrberger Strasse, Homburg, 66424, Germany ²²Department of Neuropathology, Institute of Pathology, Würzburg University Josef-Schneider Strasse 2, Würzburg, 97080, Germany ²³Department of Neurosurgery, Heidelberg University Hospital, Im Neuenheimer Feld 400, Heidelberg, 69120, Germany ²⁴Clinical Cooperation Unit Pediatric Oncology, German Cancer Research Center (DKFZ), Im Neuenheimer Feld 280, Heidelberg, 69120, Germany ²⁵Department of Neuropathology, University of Heidelberg, Im Neuenheimer Feld 220, Heidelberg, 69120, Germany ²⁶Clinical Cooperation Unit Neuropathology, German Cancer Research Center (DKFZ), Im Neuenheimer Feld 220-221, Heidelberg, 69120, Germany ²⁷Department of Pediatric Oncology, Hematology & Immunology, Klinikum Stuttgart Olgahospital, Bismarckstrasse 8, Stuttgart, 70176, Germany ²⁸Department of Paediatric Haematology and Oncology, University Hospital Freiburg, Mathildenstrasse 1, Freiburg, 79106, Germany ²⁹Department of Hematology and Oncology, Children's University Hospital, Hoppe-Seyler Strasse 1, Tübingen, 72076, Germany ³⁰Department of Neurosurgery, University Hospital, Hoppe-Seyler Strasse 3, Tübingen, 72076, Germany ³¹Children's Hospital Augsburg, Stenglinstrasse 2, Augsburg, 86156, Germany ³²Institute of Neuropathology, University Hospital Münster, Albert-Schweitzer-Campus 1, Münster, 48149, Germany ³³Departments of Pediatrics and Human Genetics, McGill University and the McGill University Health Center Research Institute, Montreal, Quebec, H3Z 2Z3, Canada ³⁴Department of Paediatric Haematology and Oncology, University Medical Center Hamburg-Eppendorf, Martinistrasse 52, Hamburg, 20246, Germany ³⁵Northern Institute for Cancer Research, Newcastle University, Royal Victoria Infirmary, Newcastle-upon-Tyne, NE1 4LP, UK ³⁶School of Cancer and Enabling Sciences, University of Manchester, Manchester Academic Health Science Centre, Manchester, M13 9PL, UK ³⁷Division of Molecular Histopathology, Department of Pathology, University of Cambridge, Cambridge, CB2 0QQ, UK ³⁸Division of Molecular Genome Analysis, German Cancer Research Center (DKFZ), Im Neuenheimer Feld 280, Heidelberg, 69120, Germany ³⁹Cnopfsche Kinderklinik, Nürnberg Children's Hospital, St.-Johannis-Mühlgasse 19, Nürnberg, 90419, Germany ⁴⁰Department of Neuropathology, Heinrich-Heine-University Düsseldorf, Moorenstrasse 5, Düsseldorf, 40225, Germany ⁴¹Division of Neurosurgery and The Arthur and Sonia Labatt Brain Tumour Research Centre, Hospital for Sick Children, 555

University Avenue, Toronto, Ontario, M5G 1X8, Canada ⁴²Dana Farber Cancer Institute, 450 Brookline Avenue, Boston, MA, 02215, USA ⁴³Children's Hospital Boston, 300 Longwood Avenue, Boston, MA, 02115, USA ⁴⁴Institute of Pharmacy and Molecular Biotechnology, and Bioquant Center, University of Heidelberg, Im Neuenheimer Feld 267, Heidelberg, 69120, Germany ⁴⁵<http://www.pedbraintumor.org>

Summary

Medulloblastoma is an aggressively-growing tumour, arising in the cerebellum or medulla/brain stem. It is the most common malignant brain tumour in children, and displays tremendous biological and clinical heterogeneity¹. Despite recent treatment advances, approximately 40% of children experience tumour recurrence, and 30% will die from their disease. Those who survive often have a significantly reduced quality of life.

Four tumour subgroups with distinct clinical, biological and genetic profiles are currently discriminated^{2,3}. WNT tumours, displaying activated wingless pathway signalling, carry a favourable prognosis under current treatment regimens⁴. SHH tumours show hedgehog pathway activation, and have an intermediate prognosis². Group 3 & 4 tumours are molecularly less well-characterised, and also present the greatest clinical challenges^{2,3,5}. The full repertoire of genetic events driving this distinction, however, remains unclear.

Here we describe an integrative deep-sequencing analysis of 125 tumour-normal pairs. Tetraploidy was identified as a frequent early event in Group 3 & 4 tumours, and a positive correlation between patient age and mutation rate was observed. Several recurrent mutations were identified, both in known medulloblastoma-related genes (*CTNNB1*, *PTCH1*, *MLL2*, *SMARCA4*) and in genes not previously linked to this tumour (*DDX3X*, *CTDNEP1*, *KDM6A*, *TBR1*), often in subgroup-specific patterns. RNA-sequencing confirmed these alterations, and revealed the expression of the first medulloblastoma fusion genes. Chromatin modifiers were frequently altered across all subgroups.

These findings enhance our understanding of the genomic complexity and heterogeneity underlying medulloblastoma, and provide several potential targets for new therapeutics, especially for Group 3 & 4 patients.

As a first phase of the International Cancer Genome Consortium (ICGC) PedBrain Tumor Project (www.pedbraintumor.org), we have collected matched tumour and germline samples from 125 medulloblastoma patients aged from 0–17 years (Supplementary Table 1). Whole-genome sequencing (WGS, n=39) and whole-exome sequencing (WES, n=21) were applied to a 'Discovery' set, with a custom-capture approach used to sequence 2,734 genes in an additional 'Replication' set (n=65). All tumour samples were obtained at primary diagnosis, prior to adjuvant therapy, and the distribution of molecular subgroups was similar across cohorts (Supplementary Figure 1).

Investigation of genome-wide somatic mutation allele frequencies identified several cases with a clear peak at ~25%, rather than the expected ~50% allele frequency for early, heterozygous events (Figure 1a). Analysis of coverage depth and allele frequencies in regions of copy-number change ruled out stromal contamination, but rather suggested a tetraploid baseline in the tumour genome (Figure 1b). Predicted ploidy status was confirmed by fluorescence *in situ* hybridisation (FISH) using multiple centromeric probes in 17/18 cases analysed (Figure 1a). The extremely low fraction of mutations at ~50% allele frequency suggests that genome duplication occurred very early during tumourigenesis. Some cases likely went through even higher polyploidy states before reaching a ~4n baseline (e.g. ICGC_MB45, displaying 4n chromosomes with 4:0 or 3:1 allele ratios;

Supplementary Figure 2). Across the Discovery set, tetraploidy was most commonly observed in Group 3 (7/13, 54%) and Group 4 tumours (8/20, 40%), followed by SHH (4/14, 29%) and WNT tumours (1/7, 14%). Interestingly, the four tetraploid SHH tumours all harboured *TP53* mutations and also displayed chromothripsis⁶. Tetraploid Group 3 & 4 tumours showed significantly more large-scale copy number alterations compared with diploid cases (median 10 changes per tumour in tetraploid versus 4 per tumour in diploid cases, $p=0.008$, two-tailed Mann-Whitney U test; Supplementary Figure 3). Thus, tetraploidy followed by genomic instability may be an early driving event in a large proportion of Group 3 & 4 medulloblastomas, which pose a significant clinical challenge due to their dismal prognosis and lack of targeted treatment options. Novel classes of drugs such as mitotic checkpoint kinase or kinesin inhibitors, which target the maintenance of tetraploidy through successive cell divisions, may therefore represent a rational therapeutic strategy in these cases^{7,8}. The value of tetraploidy as a prognostic marker also requires further investigation.

The average somatic mutation rate in the WGS cohort was 0.52/Mb, with an average of 10.3 non-synonymous coding single nucleotide variants (SNVs) in the Discovery cohort (Supplementary Table 2). This is slightly higher than previously reported for medulloblastoma⁹, possibly due to improved coverage and technical sensitivity, but considerably lower than in deep-sequenced adult tumours, e.g.^{10,11}. There were significantly fewer transitions in the somatic alterations compared with germline variation ($p=4.6\times 10^{-7}$, Wilcoxon rank-sum test; Supplementary Figure 4). All coding somatic SNVs identified in the combined cohort are listed in Supplementary Table 3.

We identified a positive correlation between genome-wide mutation rate and patient age, as previously reported for coding mutations⁹ ($r^2 = 0.35$, $p=7.8\times 10^{-5}$ Pearson's product-moment correlation; Figure 1c). Intriguingly, this association was more pronounced in diploid tumours ($r^2 = 0.52$, $p=3\times 10^{-5}$), and virtually absent in tetraploid cases ($r^2 = 0.04$, $p=0.5$) (Supplementary Figure 5a,b). A similar trend was observed for non-synonymous mutations across the Discovery cohort (Supplementary Figure 5c). Coverage level did not correlate with mutation rate (Supplementary Figure 5d). One explanation may be that all medulloblastomas originate during embryogenesis, with some tumours needing to accumulate more genetic 'hits' before becoming symptomatic. Alternatively, tumours arising in older patients may derive from more differentiated cells that require a greater number of alterations to undergo malignant transformation. Investigation of additional tumours from older patients may help to clarify this.

Five SHH tumours harbouring *TP53* mutations, including three previously described Li-Fraumeni syndrome (LFS)-associated tumours with germline mutations⁶, one newly-identified LFS case (ICGC_MB23), and one somatically mutated tumour (ICGC_MB34), had significantly more mutations than the remaining cases, both genome wide (mean 1.1/Mb vs 0.43/Mb, $p=4.5\times 10^{-6}$; two-tailed t-test) and for non-synonymous changes (mean 23 vs 8.8, $p=2.6\times 10^{-6}$). Interestingly, the WNT subgroup, which typically shows a good prognosis and few copy-number changes, had the next highest mutation rate (Figure 1d).

Forty-one somatic, coding, small insertions/deletions (InDels) were identified across the cohort, with an average of 0.4 coding InDels per case in the Discovery set (range 0–2; Supplementary Table 4). Some genes, however, were more commonly affected by InDels than SNVs. For example, frameshift InDels in *PTCH1* were detected in 6/125 cases, while only 2 SNVs were observed. Recurrent InDels were also seen in the chromatin modifiers *MLL2*, *KDM6A* (3 cases each) and *BCOR* (2 cases).

In contrast to another paediatric brain tumour, glioblastoma, in which we recently identified frequently recurrent hotspot mutations¹², the majority of mutated genes in this study were unique to a single case (587/760 non-synonymous SNVs in the 125 cases, 77%) - demonstrating the pronounced genetic heterogeneity of medulloblastoma. Twenty-five of these singleton mutations, and 53 SNVs in total, were at positions listed in the COSMIC database of somatic alterations in tumours (available at <http://www.sanger.ac.uk/genetics/CGP/cosmic/>), suggesting a rare but important contribution of many known cancer genes in MB (Supplementary Table 5). Only 8 genes were somatically altered in more than 3% of the whole series: *CTNNB1* (15 cases, 12%); *DDX3X* (10 cases, 8%); *PTCH1* (8 cases, 6%), *SMARCA4* (6 cases, 5%), *MLL2* (6 cases, 5%), *TP53* (somatically mutated in 5 cases, 4%), *KDM6A* (5 cases, 4%) and *CTDNEP1* (4 cases, 3%) (Figure 2). These were also the only genes found to be significantly altered upon analysis of the combined cohort with MutSig - an algorithm testing whether the observed mutations in a gene are not simply a consequence of random background mutation processes. It takes into account gene length and composition, silent to non-silent mutation ratios, and other factors (see <https://confluence.broadinstitute.org/display/CGATools/MutSig>; Supplementary Table 6). Large-scale copy-number changes known to be associated with medulloblastoma, such as formation of an isodicentric 17q and losses of 10q / 9q / X¹³⁻¹⁵, were more frequently recurrent than SNVs (Supplementary Figure 6a-e).

Many alterations were enriched in specific medulloblastoma subgroups. For example, all of the WNT tumours (15/15) harboured a mutation in *CTNNB1*, and 13/15 displayed loss of one copy of chromosome 6 (or acquired uniparental disomy in one case) - alterations which have previously been associated with this subgroup^{4,13,15}. Mutations in *DDX3X* were also clearly enriched in WNT tumours (adjusted $p=7.06 \times 10^{-6}$, two-tailed Fisher's exact test with a Bonferroni correction), and these mutations were clustered within the helicase domain (Supplementary Figure 7a). Three were localised at the RNA binding surface of the protein and three were predicted to disrupt the closed (RNA binding) conformation (Supplementary Figure 7b). The remainder were predicted to indirectly disrupt either the positive charge on the RNA binding surface ($n=2$) or the folding of the closed form ($n=2$). No truncating mutations were found, suggesting an alteration rather than simply a loss of function. *DDX3X* has recently been proposed to have an oncogenic role^{10,11}, although its exact function in tumourigenesis remains to be determined.

As anticipated from previous studies^{13,16}, SHH tumours frequently showed loss of the whole of chromosome arm 9q, as well as alterations in key hedgehog-pathway signalling molecules (e.g. *PTCH1*, altered in 8 cases; *MYCN*, amplified in 5 cases, and *SMO*, mutated in ICGC_MB12).

The most frequently mutated gene in Group 3 tumours was *SMARCA4*, (3/26 cases). As with *DDX3X*, these mutations were clustered in the helicase domain (Supplementary Figure 7a). As noted above, tetraploidy was also a common event in this subgroup, and in Group 4 tumours. Recurrent truncating mutations in *KDM6A* (on chromosome X, which frequently shows copy-number loss in female Group 3 & 4 medulloblastoma patients; also known as *UTX*), encoding a histone 3 lysine 27 (H3K27) demethylase, were also seen in Group 4 (4/40, 10%), indicating a tumour suppressive role in this subgroup, as previously described for other cancers¹⁷. *CTDNEP1* (a homologue of the *Xenopus* gene *DULLARD*), was also affected by truncating alterations in four tumours. In three of these cases, the mutation was accompanied by loss of the wild-type allele through isodicentric 17q formation. This gene, encoding a nuclear envelope phosphatase, was shown in *Xenopus* to have roles in BMP signalling and neural development¹⁸. In mammalian cells it is involved in the lipid activation pathway, regulating nuclear membrane biogenesis and production of diacylglycerol^{19,20}. Given the high frequency of isodicentric 17q in medulloblastoma,

genetic targets on this chromosome have long been sought after. *CTDNEP1* may be a good candidate for one of the medulloblastoma tumour suppressors on 17p.

Aside from these subgroup-enriched events, a commonly recurring theme across all medulloblastomas is alterations in genes involved in chromatin modification. Some point mutations and DNA copy number alterations in this pathway have previously been implicated in medulloblastoma^{9,21}. Overall, 45/125 cases (36%) harboured a mutation in a gene categorised under the Gene Ontology term ‘Chromatin Modification’ (GO:0015168, Supplementary Figure 6f,g).

We recently described an enrichment of catastrophic DNA rearrangements (‘chromothripsis’) in *TP53*-mutated SHH medulloblastomas⁶. Three new *TP53*-mutant SHH tumours were identified in this study: ICGC_MB23 (germline mutation), MBRep_T29 and MBRep_T53 (somatic mutations). Two of these, ICGC_MB23 and MBRep_T53, showed complex genomic rearrangements suggestive of the chromothripsis model (Supplementary Figure 8)²².

Deep sequencing also allowed fine-mapping of two amplicons on chromosome 7 in ICGC_MB34 (a SHH tumour with a somatic *TP53* mutation, relating to MB2034 in⁶). One amplicon included the entire *SHH* gene, while the second disrupted *DNAJB6*, such that its first exon was juxtaposed to *SHH* (Figure 3a,b). RNA sequencing further revealed a novel fusion transcript, not expected from the DNA data, containing the first exon of *DNAJB6* and exons 2 & 3 of *SHH*. The first exon of *SHH* was skipped, resulting in a predicted N-terminally truncated SHH protein (Figure 3c). Expression of SHH was extremely high in this case, whilst virtually absent in 301 other medulloblastomas (Supplementary Figure 9a). Predicted DNA and RNA junctions were validated by PCR (Supplementary Figure 9b).

Several additional in-frame gene fusions were identified by large insert mate-pair sequencing, which gives better resolution for structural variant detection. ICGC_MB18, for example, carried an intrachromosomal translocation resulting in a fusion between *LCLAT1* and *ERBB4*, the latter of which has previously been associated with MB oncogenesis²³ (Supplementary Figure 9c–f). In ICGC_MB6, a complex rearrangement of fragments from chromosomes 1 and 17 produced a fusion between *MLLT6* and *MRPL45*, a mitochondrial ribosomal protein, resulting in strong overexpression of the latter (Supplementary Figure 10a–c). These findings indicate that gene fusions involving well-established medulloblastoma oncogenes may play a more important role in MB than previously recognised, and warrant further investigation.

High-coverage, strand-specific RNA sequencing of 28 cases allowed us to determine the proportion of DNA SNVs that were observable in the transcriptome (Supplementary Tables 3 & 4). Overall, 129/268 (48%) non-synonymous mutations in the DNA were also detectable at the RNA level. A further 38% (101/268) resided in genes expressed at extremely low abundance (reads per kilobase of exon model per million mapped reads (RPKM) <1). Thus, the fraction of expressed mutations is even smaller than the already low number of DNA alterations, supporting the hypothesis that very few driving hits are needed to generate this paediatric tumour. It may also be the case that some mutations required for tumour initiation are not essential for later tumour cell maintenance.

RNA sequencing further revealed monoallelic expression of a heterozygous mutation in *TBR1*, producing a p.G275C change, which was also seen in a previous study⁹ (Supplementary Figure 11a). *TBR1* encodes a T-box transcription factor involved in brain development²⁴. This gene, and a second family member, *EOMES* (or *TBR2*), clearly showed subgroup-specific differential expression (Figure 4a). Sequencing of *TBR1* exon 2 in a further 85 medulloblastomas revealed one additional case with an identical mutation.

All three mutated tumours were in Group 4. Gene expression was also strongly correlated with DNA methylation for both *TBR1* and *EOMES* (Figure 4b,c, Supplementary Figure 11b,c), and expression of *TBR1* and *EOMES* is inversely correlated in Group 4 tumours (Figure 4d), giving subsets that are either *TBR1*-methylated and *EOMES*^{hi} or *EOMES*-methylated and *TBR1*^{hi} (Supplementary Figure 11d,e). These two genes are markers for different stages of neuronal lineage commitment, suggesting possible differences in cell-of-origin or differentiation within Group 4 subpopulations²⁵.

This large, integrative genomics study has provided a detailed insight into new mechanisms contributing to medulloblastoma tumourigenesis and disclose novel targets for therapeutic approaches, especially for Group 3 & 4 patients. The molecular subgroup-related enrichment of many alterations highlights the importance of considering this distinguishing factor in research, trial design and clinical practice.

Methods Summary

All patient material was collected after receiving informed consent according to ICGC guidelines and as approved by the institutional review board of contributing centres. Tumour subgrouping was based on gene expression profiling or immunohistochemical analysis as described by Northcott *et al*⁶.

Next generation sequencing was performed using Illumina technologies. Mean DNA sequence coverage was 35-fold for whole-genome cases (range 26–56×), while mean on-target coverage in the whole-exome and replication cohorts was 68-fold (74% of targets above 20× for whole-exome, 66% for the replication cohort). Exome capture was carried out with Agilent SureSelect (Human All Exon 50 Mb and XT Custom Library) in-solution reagents. Sequence data were aligned to the hg19 human reference genome assembly; duplicate and non-uniquely mapping reads were excluded. Tumour ploidy was predicted from sequencing data by a novel approach integrating copy number aberrations with allele frequencies. A subset of sequence variants were validated using PCR and Sanger sequencing. Verification rates were 95% (128/135) for SNVs and 100% (14/14) for InDels (Supplementary Tables 3 and 4). A complete description of the materials and methods is provided in the Supplementary Information.

Supplementary Material

Refer to Web version on PubMed Central for supplementary material.

Acknowledgments

We thank GATC Biotech AG for sequencing services. For technical support and expertise we thank: Bettina Haase, Dinko Pavlinic, and Bianka Baying from the EMBL Genomics Core facility; Michael Wahlers and Rupert Lück from the EMBL high-performance computing facility; the DKFZ Genomics and Proteomics Core Facility; Ina Kutschera from the NCT Heidelberg, Karin Schlangen, Macha Metsger, Kerstin Schulz, Asja Nürnberger, Alexander Kovacovics, and Matthias Linser from the Max Planck Institute for Molecular Genetics, Janet C. Lindsey, Simon Bailey and Danita M. Pearson.

This work was principally supported by the PedBrain Tumor Project contributing to the International Cancer Genome Consortium, funded by German Cancer Aid (109252) and the German Federal Ministry of Education and Research (BMBF, NGFN^{plus} #01GS0883). Additional support came from the German Cancer Research Center – Heidelberg Center for Personalized Oncology (DKFZ-HIPO), the Max Planck Society, the Pediatric Brain Tumor Foundation, the Italian Neuroblastoma Foundation and the Samantha Dickson Brain Tumour Trust. This study included samples provided by the UK Children's Cancer and Leukaemia Group (CCLG) as part of CCLG-approved biological study BS-2007-04.

References

1. Louis D, et al. The 2007 WHO Classification of Tumours of the Central Nervous System. *Acta Neuropathologica*. 2007; 114:97–109. [PubMed: 17618441]
2. Kool M, et al. Molecular subgroups of medulloblastoma: an international meta-analysis of transcriptome, genetic aberrations, and clinical data of WNT, SHH, Group 3, and Group 4 medulloblastomas. *Acta Neuropathol*. 2012; 123:473–484. [PubMed: 22358457]
3. Taylor MD, et al. Molecular subgroups of medulloblastoma: the current consensus. *Acta Neuropathol*. 2012; 123:465–472. [PubMed: 22134537]
4. Clifford S, et al. Wnt/Wingless Pathway Activation and Chromosome 6 Loss Characterise a Distinct Molecular Sub-Group of Medulloblastomas Associated with a Favourable Prognosis. *Cell Cycle*. 2006; 5:2666–2670. [PubMed: 17172831]
5. Northcott PA, et al. Medulloblastoma comprises four distinct molecular variants. *J Clin Oncol*. 2011; 29:1408–1414. [PubMed: 20823417]
6. Rausch T, et al. Genome sequencing of pediatric medulloblastoma links catastrophic DNA rearrangements with TP53 mutations. *Cell*. 2012; 148:59–71. [PubMed: 22265402]
7. Rello-Varona S, et al. Preferential killing of tetraploid tumor cells by targeting the mitotic kinesin Eg5. *Cell Cycle*. 2009; 8:1030–1035. [PubMed: 19270519]
8. Vitale I, et al. Inhibition of Chk1 kills tetraploid tumor cells through a p53-dependent pathway. *PLoS One*. 2007; 2:e1337. [PubMed: 18159231]
9. Parsons DW, et al. The Genetic Landscape of the Childhood Cancer Medulloblastoma. *Science*. 2011; 331:435–439. [PubMed: 21163964]
10. Stransky N, et al. The mutational landscape of head and neck squamous cell carcinoma. *Science*. 2011; 333:1157–1160. [PubMed: 21798893]
11. Wang L, et al. SF3B1 and other novel cancer genes in chronic lymphocytic leukemia. *N Engl J Med*. 2011; 365:2497–2506. [PubMed: 22150006]
12. Schwartzentruber J, et al. Driver mutations in histone H3.3 and chromatin remodelling genes in paediatric glioblastoma. *Nature*. 2012; 482:226–231. [PubMed: 22286061]
13. Kool M, et al. Integrated Genomics Identifies Five Medulloblastoma Subtypes with Distinct Genetic Profiles, Pathway Signatures and Clinicopathological Features. *PLoS ONE*. 2008; 3:e3088. [PubMed: 18769486]
14. Pfister S, et al. Outcome prediction in pediatric medulloblastoma based on DNA copynumber aberrations of chromosomes 6q and 17q and the MYC and MYCN loci. *J Clin Oncol*. 2009; 27:1627–1636. [PubMed: 19255330]
15. Thompson MC, et al. Genomics identifies medulloblastoma subgroups that are enriched for specific genetic alterations. *J Clin Oncol*. 2006; 24:1924–1931. [PubMed: 16567768]
16. Pietsch T, et al. Medulloblastomas of the Desmoplastic Variant Carry Mutations of the Human Homologue of *Drosophila patched*. *Cancer Res*. 1997; 57:2085–2088. [PubMed: 9187099]
17. van Haaften G, et al. Somatic mutations of the histone H3K27 demethylase gene UTX in human cancer. *Nat Genet*. 2009; 41:521–523. [PubMed: 19330029]
18. Satow R, Kurisaki A, Chan TC, Hamazaki TS, Asashima M. Dullard promotes degradation and dephosphorylation of BMP receptors and is required for neural induction. *Dev Cell*. 2006; 11:763–774. [PubMed: 17141153]
19. Han S, et al. Nuclear envelope phosphatase 1-regulatory subunit 1 (formerly TMEM188) is the metazoan Spo7p ortholog and functions in the lipin activation pathway. *J Biol Chem*. 2012; 287:3123–3137. [PubMed: 22134922]
20. Kim Y, et al. A conserved phosphatase cascade that regulates nuclear membrane biogenesis. *Proc Natl Acad Sci U S A*. 2007; 104:6596–6601. [PubMed: 17420445]
21. Northcott PA, et al. Multiple recurrent genetic events converge on control of histone lysine methylation in medulloblastoma. *Nat Genet*. 2009; 41:465–472. [PubMed: 19270706]
22. Stephens PJ, et al. Massive Genomic Rearrangement Acquired in a Single Catastrophic Event during Cancer Development. *Cell*. 2011; 144:27–40. [PubMed: 21215367]

23. Gilbertson RJ, Perry RH, Kelly PJ, Pearson ADJ, Lunec J. Prognostic Significance of HER2 and HER4 Coexpression in Childhood Medulloblastoma. *Cancer Res.* 1997; 57:3272–3280. [PubMed: 9242460]
24. Hevner RF, et al. Tbr1 regulates differentiation of the preplate and layer 6. *Neuron.* 2001; 29:353–366. [PubMed: 11239428]
25. Englund C, et al. Pax6, Tbr2, and Tbr1 are expressed sequentially by radial glia, intermediate progenitor cells, and postmitotic neurons in developing neocortex. *J Neurosci.* 2005; 25:247–251. [PubMed: 15634788]

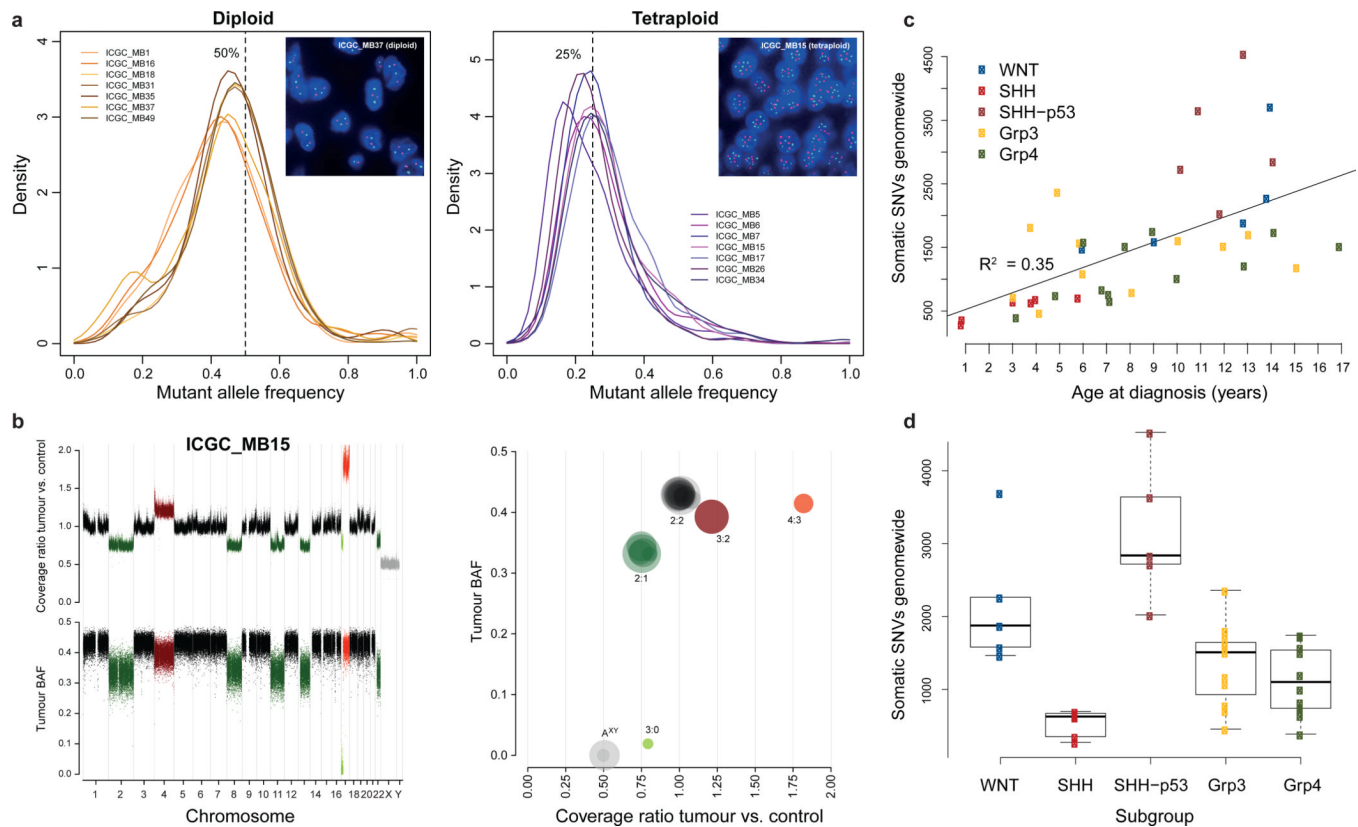


Figure 1. Tetraploidy is a frequent early event in MB tumorigenesis, and mutation rates vary with age and subgroup

a, Distributions of genome-wide somatic mutation allele frequencies (the proportion of sequence reads supporting a mutation) for diploid tumours (with a peak at ~50% for heterozygous events, $n=7$) and tetraploid cases (with a peak at ~25%, $n=7$). Insets show centromeric FISH for chromosomes 1 (red) and 11 (green), confirming the predicted ploidy status.

b, Top left: Rescaled tumour:germline coverage ratio, indicating copy-number gains (red) or losses (green). Bottom left: B-Allele frequency (BAF) in the tumour at SNP positions which are heterozygous in the germline. Right: Genome alteration print (GAP) of segmented copy number and allele frequency profiles. Chromosomes with predicted 3:0/2:1/3:2 allele ratios show a BAF of ~0/0.33/0.4 and coverage ratios of ~0.75/0.75/1.25. Due to random sampling, the 2:2 allele ratio is slightly below 0.5.

c, Genome-wide somatic mutation rates are positively correlated with patient age ($n=39$).

d, Distribution of somatic mutation rates by tumour subgroup ($n=39$). p-values are according to a Wilcoxon rank-sum test with Bonferroni correction. SHH-p53: SHH-subgroup tumours harbouring a somatic or germline *TP53* mutation.

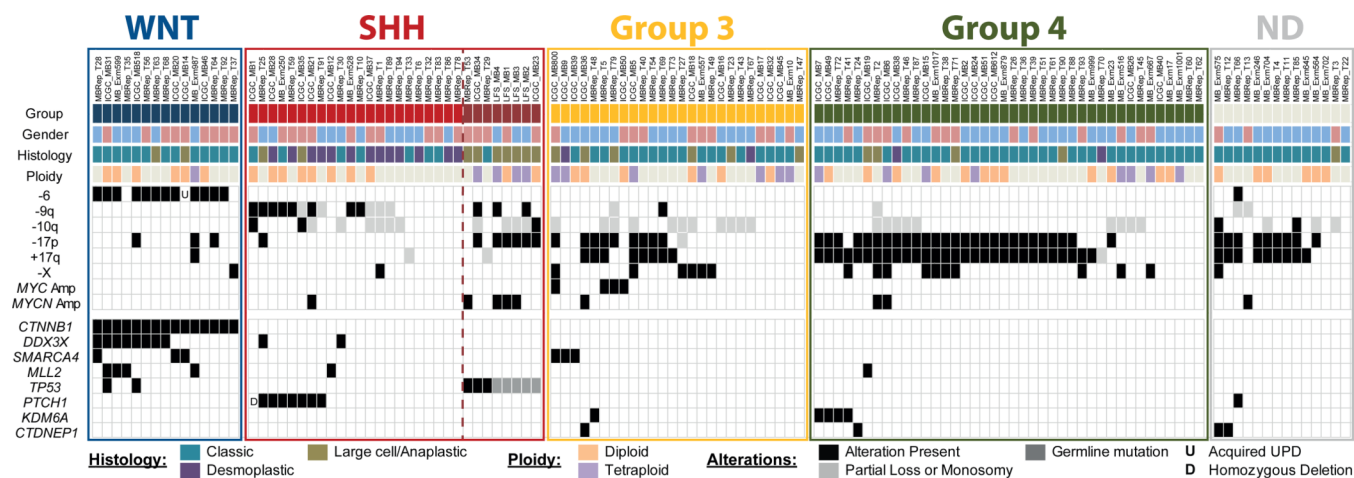


Figure 2. Subgroup specificity of common genetic alterations

Summary of clinical data and recurrent alterations in the combined cohort (n=125). Genes which were found to be significantly mutated by MutSig analysis were included. UPD: uniparental disomy, ND: no material available for conclusive molecular subgroup assignment.

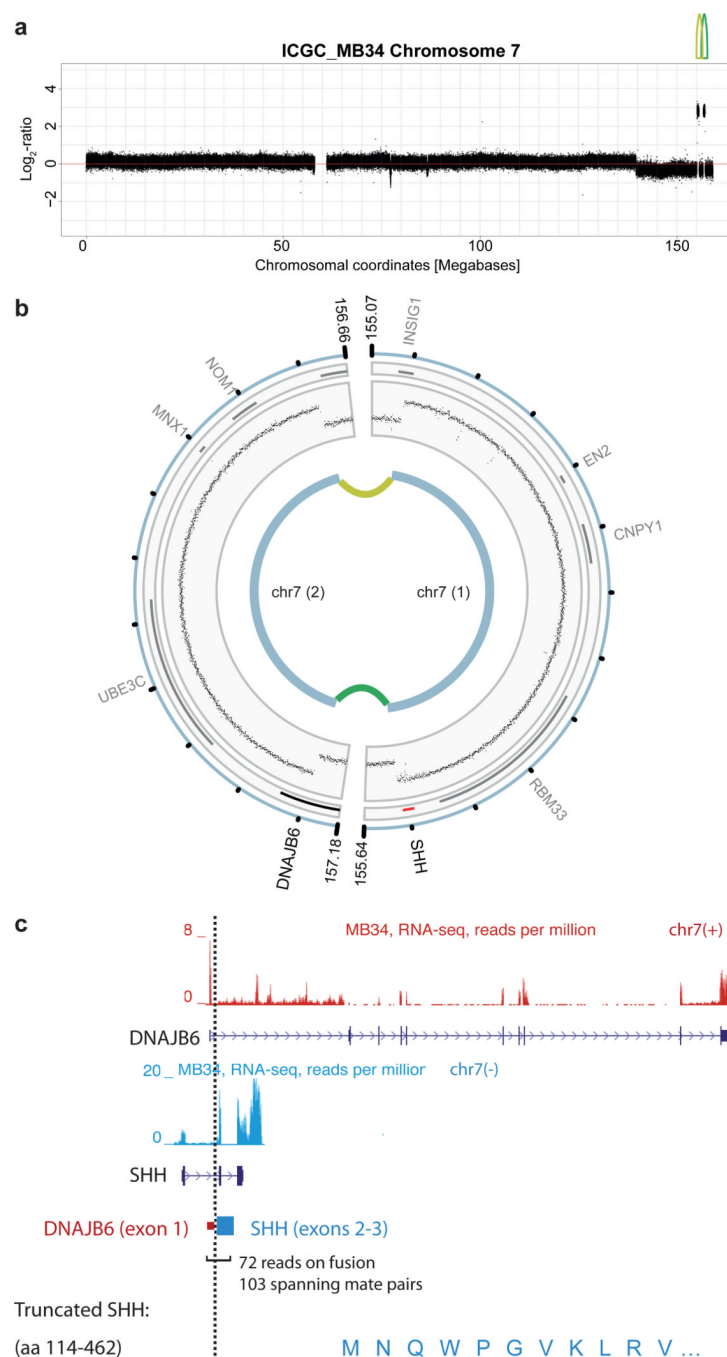


Figure 3. Identification of novel fusion genes in MB

a, Read-depth plot with log₂ tumour:germline coverage ratio showing alterations on chromosome 7 in ICGC_MB34. Lines indicate connected segments.

b, Schematic of the rearrangement.

c, Details of the *SHH* fusion gene structure and support for its expression, derived from RNA sequencing data.

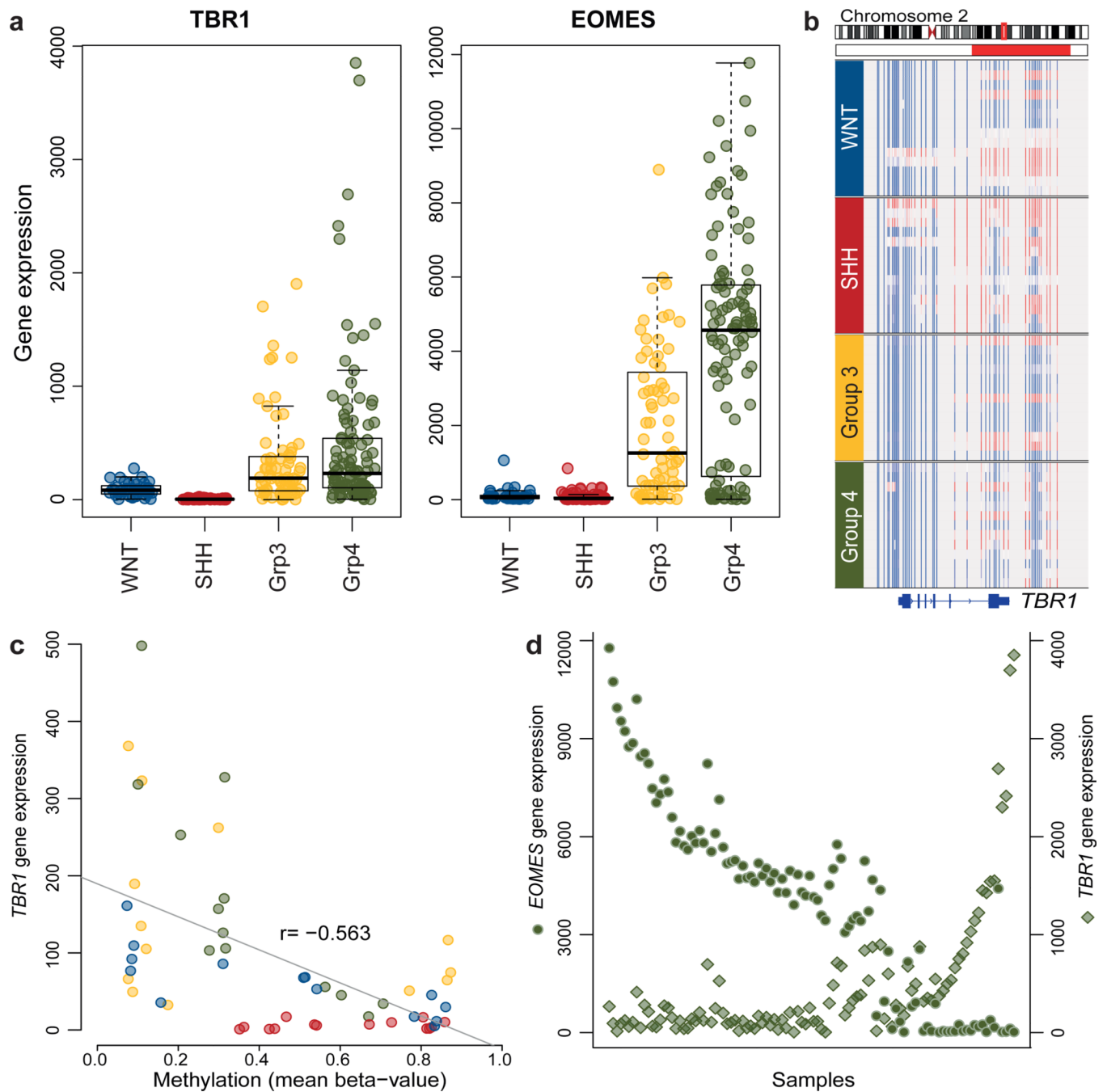


Figure 4. Integration of mutation, expression and methylation data shows differential regulation of *TBR1* and *EOMES* in medulloblastoma

a, Microarray data showing clear differences in *TBR1* and *EOMES* expression between medulloblastoma subgroups (n=301).

b, DNA methylation of *TBR1* (n=54), ranging from low (blue) to high (red). Horizontal red bar indicates the region used for correlation analysis in **c**.

c, Expression of *TBR1* is tightly correlated with gene methylation (n=54; Pearson's correlation values, r). SHH tumours show high methylation and virtually no expression, while WNT, Group 3 and Group 4 tumours display a more varied pattern.

d, Expression levels of *TBR1* (diamonds) and *EOMES* (circles) are inversely related in Group 4 tumours (n=104).